JVI Journals.ASM.org

Differential Reovirus-Specific and Herpesvirus-Specific Activator Protein 1 Activation of Secretogranin II Leads to Altered Virus Secretion

Alicia R. Berard,[a,b] Alberto Severini,[a,c] Kevin M. Coombs[a,b,d]

Department of Medical Microbiology, Faculty of Medicine, University of Manitoba, Winnipeg, MB, Canada[a]; Manitoba Center for Proteomics and Systems Biology, John Buhler Research Center, University of Manitoba, Winnipeg, MB, Canada[b]; National Microbiology Laboratory, Public Health Agency of Canada, Winnipeg, MB, Canada[c]; Manitoba Institute of Child Health, University of Manitoba, Winnipeg, MB, Canada[d]

ABSTRACT

Viruses utilize host cell machinery for propagation and manage to evade cellular host defense mechanisms in the process. Much remains unknown regarding how the host responds to viral infection. We recently performed global proteomic screens of mammalian reovirus TIL- and T3D-infected and herpesvirus (herpes simplex virus 1 [HSV-1])-infected HEK293 cells. The nonenveloped RNA reoviruses caused an upregulation, whereas the enveloped DNA HSV-1 caused a downregulation, of cellular secretogranin II (SCG2). SCG2, a member of the granin family that functions in hormonal peptide sorting into secretory vesicles, has not been linked to virus infections previously. We confirmed SCG2 upregulation and found SCG2 phosphorylation by 18 h postinfection (hpi) in reovirus-infected cells. We also found a decrease in the amount of reovirus secretion from SCG2 knockdown cells. Similar analyses of cells infected with HSV-1 showed an increase in the amount of secreted virus. Analysis of the stress-activated protein kinase (SAPK)/Jun N-terminal protein kinase (JNK) pathway indicated that each virus activates different pathways leading to activator protein 1 (AP-1) activation, which is the known SCG2 transcription activator. We conclude from these experiments that the negative correlation between SCG2 quantity and virus secretion for both viruses indicates a virus-specific role for SCG2 during infection.

IMPORTANCE

Mammalian reoviruses affect the gastrointestinal system or cause respiratory infections in humans. Recent work has shown that all mammalian reovirus strains (most specifically T3D) may be useful oncolytic agents. The ubiquitous herpes simplex viruses cause common sores in mucosal areas of their host and have coevolved with hosts over many years. Both of these virus species are prototypical representatives of their viral families, and investigation of these viruses can lead to further knowledge of how they and the other more pathogenic members of their respective families interact with the host. Here we show that secretogranin II (SCG2), a protein not previously studied in the context of virus infections, alters virus output in a virus-specific manner and that the quantity of SCG2 is inversely related to amounts of infectious-virus secretion. Herpesviruses may target this protein to facilitate enhanced virus release from the host.

Viruses that infect a host cell rely on the host machinery to replicate while managing to evade the immune system. Thus, there is an intricate relationship between the host and the virus that can be characterized by measuring changes in the host's protein effector molecules during the course of infection. In a previous study (1), we identified numerous HEK293 protein abundance changes after infection with the prototypic mammalian reovirus subtype 1 Lang (T1L), including the upregulation of secretogranin II (SCG2) at 24 h postinfection (hpi).

SCG2 is a protein in the structurally and functionally related granin family that also includes chromogranins A and B, secretogranin III, secretogranin V (secretory granule, neuroendocrine protein 1), secretogranin VI (guanine nucleotide binding protein [G protein], alpha-stimulating-activity polypeptide 1 [GNAS1]), secretogranin VII (VGF; nonacronym name), and secretogranin VIII (proprotein convertase subtilisin/kexin type 1 inhibitor [PCSK1N]) (2). Granins are acidic proteins that are found in secretory vesicles where they bind to calcium, are heat stable, are soluble, can aggregate, and are generally larger than classical peptide precursors (2, 3). Members of the granin family have functions in the packaging of hormones, growth factors, enzymes, and catecholamines in large dense-core vesicles (4). Granins are precursor proteins of several different bioactive peptides that are also involved in hormone release and secretory granule formation (3).

SCG2 was first characterized in anterior pituitary cells. However, it has since been located in mammalian brain, pituitary glands, gonads, adrenal glands, intestine, stomach, and pancreas (3). SCG2 is able to induce the formation of secretory granule-like structures in nonneuroendocrine cells, indicating a crucial role of SCG2 in generating secretory vesicles, and functions in the packaging and sorting of peptide hormones and neuropeptides into secretory vesicles (5). Two domains on the SCG2 full-length protein (domain spanning human SCG2 residues 25 to 41 [$hSCG2_{25-41}$] and $hSCG2_{334-348}$) are target-

Received 25 June 2015 **Accepted** 10 September 2015

Accepted manuscript posted online 16 September 2015

Citation Berard AR, Severini A, Coombs KM. 2015. Differential reovirus-specific and herpesvirus-specific activator protein 1 activation of secretogranin II leads to altered virus secretion. J Virol 89:11954–11964. doi:10.1128/JVI.01639-15.

Editor: T. S. Dermody

Address correspondence to Kevin M. Coombs, kevin.coombs@umanitoba.ca.

ing signals for sorting of the protein into regulated secretory pathway granules (6). The full-length mammalian SCG2 protein contains 617 residues and is cleaved to generate three bioactive peptides: secretoneurin (SN) (rat $SgII_{154–186}$), EM66 (rat $SgII_{189–256}$), and manserin (rat $SgII_{529–568}$) (4, 7). SN functions in stimulating luteinizing hormone secretion; stimulates neurotransmitter release; stimulates monocyte and endothelial cell migration, contributing to hypertension; stimulates inflammation; and can be detected in the cerebrospinal fluid (2, 3). EM66 participates in the control of intake (4, 8), and manserin is involved in the stress response (9).

An abundance of natural antimicrobials have been derived from granins, specifically chromogranin A (CgA) and CgB (4). Antibacterial activity has also been reported for CgA and CgB (4). A recent study of bovine and human antimicrobial chromogranin-derived peptides isolated antimicrobial peptides from the bovine SCG2 protein, namely, Rrf and Kvk, that demonstrate a role in innate immunity (10) and indicated similar peptides in the human SCG2 protein. However, to date, no one has reported a functional role of the full-length SCG2 protein, or its cleaved signaling peptides, in viral infections. Because of the potential role that SCG2 packaging and antimicrobial functions have in viral infections as well as our previous observation that SCG2 is upregulated during mammalian reovirus infection, we hypothesize that this protein plays a role during infection.

MATERIALS AND METHODS

Cells and viruses. Mouse L929 cells were maintained in Joklik's suspension-modified minimal essential medium (J-MEM) (Gibco Products, Grand Island, NY, USA) supplemented with 5% fetal bovine serum (FBS) and 200 mM L-glutamine, as previously described (11).

HEK293 (Human embryonic kidney) cells were grown in DMEM (Dulbecco's modified Eagle medium) supplemented to contain 10% FBS and 1% each L-glutamine, nonessential amino acids, and sodium pyruvate.

Vero cells were grown in DMEM supplemented to contain 10% FBS and 1% each of L-glutamine, nonessential amino acids, and sodium pyruvate.

Reovirus serotype 1 Lang (T1L), serotype 3 Dearing Fields ($T3D^F$), and serotype 3 Dearing Cashdollar ($T3D^C$) and herpes simplex virus 1 (HSV-1) (strain F) were all grown from laboratory stocks.

Infections. Approximately 10^7 HEK293 cells in T75 flasks or P100 dishes or $\sim 6 \times 10^5$ cells in each well of 12-well plates were infected with either reovirus or HSV-1 at a multiplicity of infection (MOI) of 0.1 or 5 PFU per cell, as specified below. Equivalent numbers of cells were mock infected as a control. The dishes, flasks, and plates were incubated at 4°C for 1 h, with gentle rocking every 10 to 15 min, to allow virus to adsorb and to synchronize infections. An overlay of 10 ml of prewarmed appropriate complete cell medium was then added to each dish/flask, or 1 ml was added to each well, and the infected cell cultures were incubated at 37°C for various periods of time.

Titration. The titers of reovirus samples were determined by plaque assays as previously described (11). Briefly, samples were serially diluted and used to infect 12-well plates of L929 cells and then overlaid with a 1:1 mixture of 2% agar–2× M199 medium. Plates were fed with the same overlay 3 days later.

The titers of HSV samples were similarly determined but on Vero cells. The overlay consisted of one-half 2% agar solution and one-half HSV–2× DMEM. HSV-1 plates were incubated at 37°C for 3 days.

After 3 days for HSV-1 or 7 days for reoviruses, the wells were fixed with formaldehyde and stained by using crystal violet to visualize plaques.

Immunofluorescence microscopy. HEK293 cells were mounted onto autoclaved 12-spot slides, letting the cells adhere to the slides overnight at 37°C. Once adhered, the spots were washed two times with 1× phosphate-buffered saline (PBS). The cells were counted, and virus was added to each spot at an MOI of 5 in serum-free medium. The virus was allowed to adsorb to the cells for 1 h on ice, to ensure synchronization of the infection, and complete medium was then used for the overlay. The spots were incubated for 6, 12, 18, and 24 h at 37°C. At each time point, spots were washed three times with PBS and fixed with 10% paraformaldehyde for ~15 min.

Once fixed, all spots were washed, and cells were permeabilized with 0.2% Triton X-100 for 5 min. Spots were blocked by using PBS with 1% bovine serum albumin (BSA) and 5% FBS, followed by in-house rabbit antireovirus primary antibodies; mouse anti-SCG2 (catalog number ab20245; Abcam); and then the secondary antibodies Alexa Fluor 488 goat anti-mouse (catalog number A11001; Invitrogen), Cy3 goat anti-rabbit, and 4′,6-diamidino-2-phenylindole (DAPI) (catalog number D1306; Invitrogen). Antifade reagent (catalog number P36935; Invitrogen) was added to each spot before slides were covered with coverslips. Slides were examined on a Zeiss Axio Observer Z1 inverted microscope at a ×200 magnification with fluorescence illumination using Exfo Xcite. Images were acquired by using AxioVision 4.8.2 software.

Immunoblotting. Western blot analyses of infected HEK293 cells were performed as described previously (12). Briefly, infected HEK293 cells were harvested at the specified times postinfection, washed three times with PBS, and then lysed by using 0.5% NP-40 with protease inhibitors. The cytosol was collected into separate microtubes and tested for protein concentrations by a Pierce bicinchoninic acid (BCA) protein assay kit (Thermo Scientific). Cytosolic proteins were resolved on 10% SDS-PAGE gels at 120 V for 70 min. Proteins were then transferred onto polyvinylidene difluoride (PVDF) membranes at 100 V for 60 min, and the transfers were confirmed by using Ponceau S staining. The membranes were blocked by using 5% skim milk in Tris-buffered saline–Tween (TBST) and probed by using various rabbit antibodies in 1% BSA in TBST. Primary antibodies used were in-house antireovirus, anti-SCG2 (from Abnova [catalog number PAB17107] and Pierce [catalog number PA1-10838]), antiphosphoserine antibody (catalog number ab9332; Abcam), antiphosphothreonine antibody (catalog number ab9337; Abcam), antiphosphotyrosine antibody (catalog number ab50722; Abcam), anti-glyceraldehyde-3-phosphate dehydrogenase (GAPDH) (catalog number 2118; Cell Signaling), anti-phospho-stress-activated protein kinase (SAPK)/Jun N-terminal protein kinase (JNK) (Thr183/Tyr185) (catalog number 4668; Cell Signaling), anti-phospho-SEK1/MKK4 (Ser257) (catalog number 4514; Cell Signaling), anti-phospho-ATF-2 (Thr71) (catalog number 5112; Cell Signaling), anti-phospho-c-Jun (Ser63) (catalog number 2361; Cell Signaling), and anti-SAPK/JNK (catalog number 9258; Cell Signaling). The secondary antibody used was horseradish peroxidase (HRP)-conjugated goat anti-rabbit (catalog number 7074; Cell Signaling). Bands were detected by enhanced chemiluminescence using an Alpha Innotech FluorChemQ MultiImage III instrument.

Preparation of shRNA-transduced cells. Lentivirus packaging and transduction were performed as previously described (13), using the GIPZ lentiviral vector packaging system from Open Biosystems. Briefly, plasmids were prepared by culturing *Escherichia coli* pGIPZ clones containing short hairpin microRNA-adapted RNA (shRNAmir) against the human SCG2 protein or a nontargeting shRNAmir control (catalog number RHS4346) and then isolating the plasmids by using a Qiagen Maxiprep kit. Three separate shRNAmirs were grown, targeting different sections of the human SCG2 protein (Table 1), as was one nonsense control. The plasmids were packaged into HEK293T cells, and lentivirus-containing supernatants were harvested at 48 h and 72 h posttransfection. The lentivirus collected was concentrated, and titers were determined in HEK293 cells by the presence of green fluorescent protein (GFP) colonies using a Zeiss Axio Observer Z1 inverted microscope at a ×200 magnification, with fluorescence illumination using Exfo Xcite. HEK293 cells at 30% confluence were used for transduction by the addition of lentivirus at 0.3 transforming units (TU)/cell in serum-free medium. After 6 h of incubation, complete DMEM was added to the cell cultures. At 72 h postransduction, cells were split, and fresh complete medium supplemented with 20 μg/ml puromycin to select against nontransduced cells

TABLE 1 shRNA and siRNA sequences for SCG2 mRNA

Oligonucleotide	Sequence	Abbreviation
shRNA		
V2LHS_172401	TATCTGACTCTTAGTTCTC	C10
V2LHS_172404	TAAATTGATCGTAGGACCG	F4
V2LHS_172400	CTCCTATGTATGAAGAGAA	G12
siRNA		
J-011422-05	CGACAAGGAUCAAGAAUUA	J5
J-011422-06	CCAGGAUGCUAGUUAAAUA	J6
J-011422-07	GAAGCGAGUUCCUGGUCAA	J7
J-011422-08	GCAAUUCCCUCCUAUGUAU	J8

was added. The concentration of working puromycin and length of time required to select for transduced colonies were determined by a puromycin selection kill curve according to the manufacturer's specifications (Open Biosystems).

Preparation of siRNA-transfected cells. HEK293 cells were transfected according to the Thermo Scientific DharmaFECT 1 protocol specific for HEK293 cells. Using four separate On-Target small interfering RNAs (siRNAs) against the human SCG2 protein (On-Target Plus set of 4 siRNAs, catalog identifiers J-011422-05, J-011422-06, J-011422-07, and J-011422-08) (Table 1) or an On-Target Plus nontargeting siRNA control, we determined the optimal concentration of siRNA using cell viability assays in combination with Western blot analysis to obtain the most efficient SCG2 knockdown with the best cell viability. HEK293 cells were transfected with 100 nM each On-Target siRNA or the control siRNA. The siRNA solution was prepared according to the manufacturer's instructions. Briefly, the siRNA solution was diluted in serum-free medium, and a DharmaFECT1 solution was prepared in the same serum-free medium. Both solutions were mixed together, and complete medium was added. The freshly prepared transfection medium was used on plated HEK293 cells, which were incubated for 24 h. At 24 h posttransfection, additional freshly prepared transfection medium replaced the old medium, and the cells were incubated for another 24 h. After 48 h of transfection, the cells were tested for knockdown efficiency and used for virus infection experiments.

Reovirus and HSV infections. P100 dishes were plated by using normal and control shRNA- and G12 shRNA-transfected HEK293 cells grown to ~60 to 70% confluence on the day of infection. siRNA-transfected cells were plated into 12-well plates, and various solutions were scaled accordingly. Using 1 dish/well for each cell type, for each time point (0, 6, 18, 24, and 48 hpi), and for each virus type, the cells were infected by removing the medium and adding virus at an MOI of 5 (for HSV or reovirus) or an MOI of 0.1 (for reovirus) in 2 ml cold serum-free medium per P100 dish. The virus was adsorbed for 1 h on ice, with periodic rocking of the dishes. After adsorption, 8 ml of complete DMEM was added to each dish, or 1 ml was added to each well of a 12-well plate. The dishes/wells were incubated for later times or harvested immediately for the 0-h time point. At each time point, the supernatant and cells were harvested separately into microcentrifuge tubes by scraping the cells from the dishes and spinning the cells and supernatant at 170 × *g* for 10 min. The volume of the supernatant was recorded at 0 h, and this volume was used at all other time points by the addition of double-distilled water (ddH_2O) if needed to compensate for evaporation. Aliquots of the supernatant were taken from each sample, and the cells were then washed twice with ice-cold PBS. Cells were counted, and a uniform cell count was used for all time points by adding ~3 ml of PBS to the samples and freeze-thawing cells twice to release intracellular virus into the buffer. Aliquots were taken from this solution to represent the titer of intracellular virus. Separate aliquots were also taken for Western blot analysis to ensure efficient SCG2 knockdown.

Cell viability. Cell viability was determined by a WST-1 assay (water-soluble tetrazolium salt 1; Roche) or by a trypan blue exclusion assay. The WST-1 assay was performed according to the manufacturer's protocols.

RESULTS

SCG2 is upregulated and altered by T1L infection. We previously performed a protein profiling study that identified up- and down-regulated HEK293 cell proteins after reovirus T1L infection (1). One of the proteins upregulated at 24 hpi was secretogranin II (SCG2). We initially reconfirmed this upregulation by Western blotting (Fig. 1). Different dilutions of the cell lysates were analyzed to ensure that sample overloading or overexposure of the blot did not cause apparent differences in protein abundance. An immunoreactive doublet band was also observed for the undiluted infected-cell lysate. A time course analysis showed that SCG2 upregulation started by 18 hpi, and this correlated with the occurrence of band doublets (Fig. 1Bi). Reprobing of these blots with a cocktail of antiphosphoserine, -phosphotyrosine, and -phosphothreonine antibodies showed reactivity of these, or comigrating, bands at 18, 24, and 36 hpi (Fig. 1Bii), which suggested that SCG2 was both upregulated and phosphorylated by T1L infection at late time points.

SCG2 does not colocalize with virus proteins inside the cell. Immunofluorescence microscopy of cells infected with T1L reovirus was performed at 6, 12, 18, and 24 hpi to determine the location of SCG2 during infection (Fig. 2). There was a visual increase in the amount of SCG2 in many of the infected cells by 24 hpi (Fig. 2B, red arrows), compared to uninfected cells on the same slide (yellow arrows), although some infected cells did not demonstrate increased SCG2 expression (green arrows). However, there was no consistent colocalization of SCG2 with viral proteins, and there did not appear to be a difference in the cellular location of SCG2 between infected and uninfected cells at any time point postinfection.

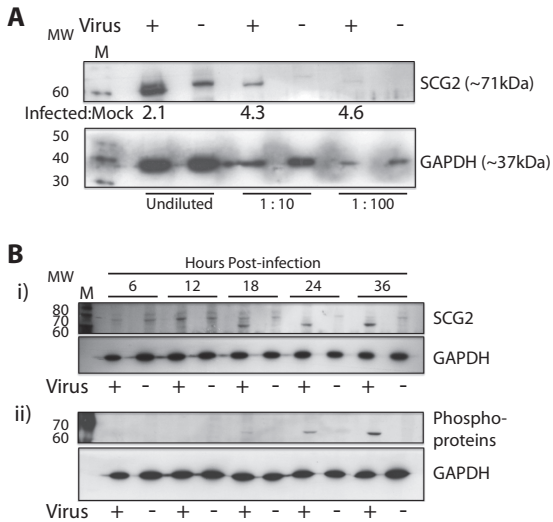

FIG 1 SCG2 expression in reovirus T1L-infected HEK293 cells at an MOI of 5. (A) Undiluted and diluted cell lysates were probed for SCG2 expression at 24 hpi. The fold increase in SCG2 expression in infected cells (+) compared to the expression level in mock, uninfected cells (−) (values below the top blot) was determined by densitometry. (B) SCG2 expression at 6, 12, 18, 24, and 36 hpi. (i) Total immunoreactive SCG2 protein; (ii) detection of phosphoproteins, using a cocktail of anti-p-Ser, anti-p-Thr, and anti-p-Tyr antibodies. MW, molecular weight (in thousands).

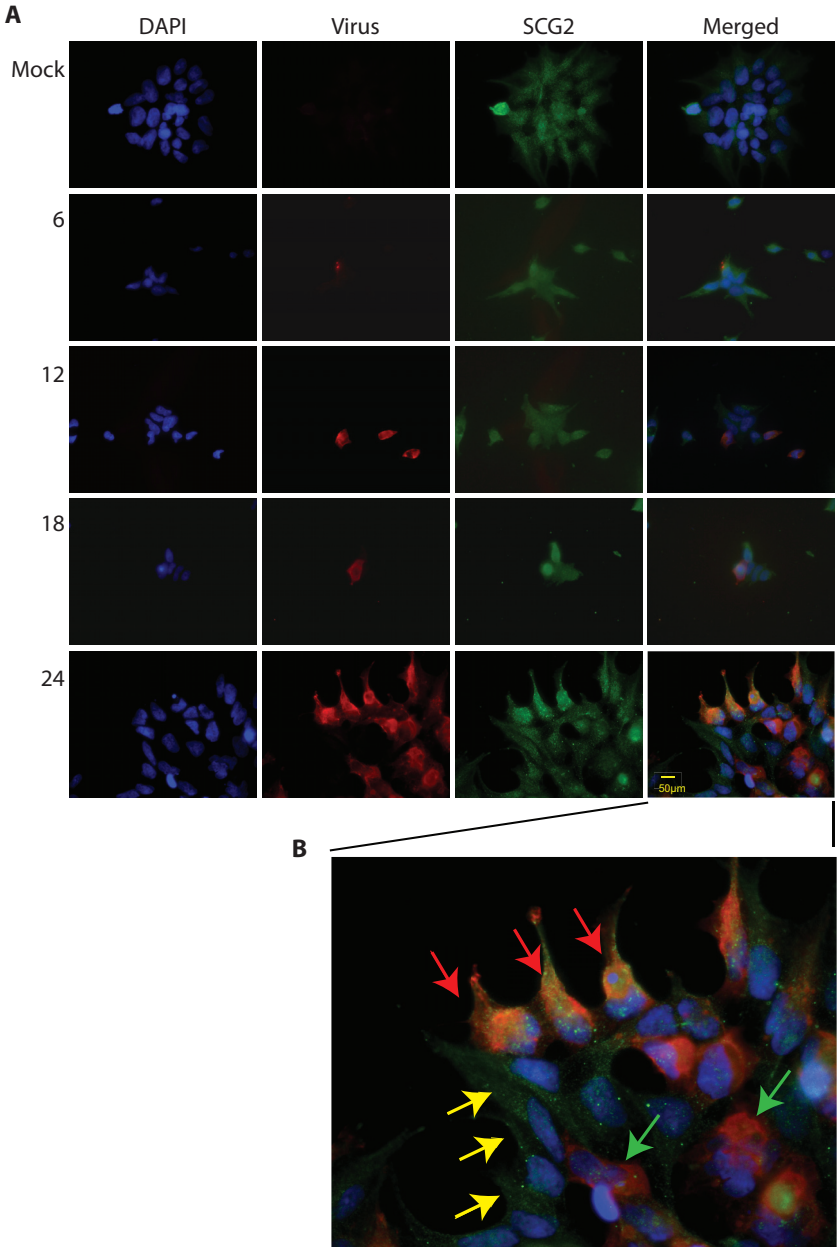

FIG 2 Immunofluorescence microscopy of the time course of SCG2 expression in T1L-infected cells. (A) Cells infected with T1L at an MOI of 5 at 6, 12, 18, and 24 hpi are shown and compared to mock-infected cells. Cells were stained with DAPI, virus was stained with Cy3 (red), and SCG2 was stained with Alexa Fluor 488 (green). (B) Enlargement of the image for the merged 24-hpi time point showing examples of infected cells with upregulated SCG2 expression (red arrows), no apparent differential SCG2 expression (green arrows), and adjacent noninfected cells (yellow arrows).

Reovirus release is reduced in SCG2 knockdown cells. Because SCG2 was upregulated after infection with T1L, we tested the possibility that the protein plays a role in infection. Three different SGC2 knockdown cells that target different locations on the protein were generated (C10, F4, and G12). SCG2 knockdown efficiency was determined by Western blotting, and densitometry indicated that expression was reduced 31%, 73%, and 66% in C10, F4, and G12 cells, respectively (Fig. 3A).

Normal, nonsilencing control, and three SCG2 knockdown cell lines were infected with T1L at two different MOIs (0.1 and 5), and samples were taken at 0, 1, 24, and 48 hpi (Fig. 3B and C). Intracellular virus titers in all five cell types were similar by 48 hpi (Fig. 3C, left). However, there was a decrease in the amount of virus that was released into the supernatant from G12 SCG2 knockdown cells at both MOIs (Fig. 3C, right). The F4 knockdown cell line had a slight decrease in the amount of virus in the supernatant at both 24 and 48 hpi at the lower MOI (Fig. 3C, upper panels) but did not maintain this decrease at 48 hpi for the higher MOI (Fig. 3C, lower panels). Although F4 cells had a similar knockdown of SCG2, they proved to be less stable than G12 cells for culturing. For this reason, G12 cells were used for further characterization of SCG2 knockdown effects.

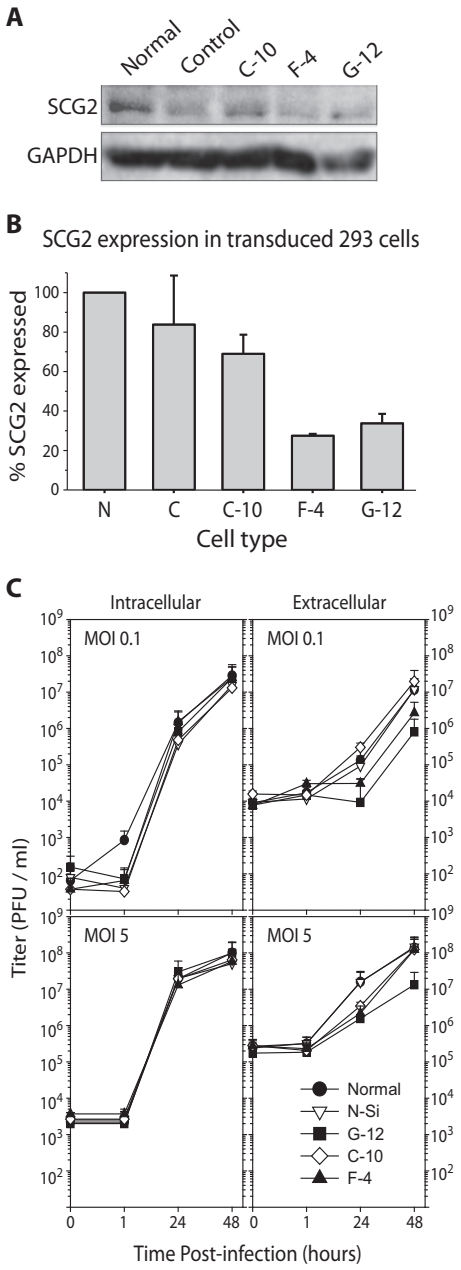

FIG 3 shRNA-mediated SCG2 knockdown. (A) Representative immunoblot of SCG2 expression compared to that of GAPDH in normal (N) HEK293 cells and in cells transduced with either a nonsilencing (N-Si) control (C) or three different SCG2 shRNA lentiviruses (C10, F4, and G12). (B) Densitometric determination of SCG2 expression levels in shRNA-transduced cells, normalized to the GAPDH levels in the same lanes and to those for mock treatment ($n = 3$, with standard errors of the means indicated by error bars). (C) Growth assays of reovirus T1L in SCG2 knockdown cells. The five different cell lines were infected with T1L at an MOI of 0.1 (top) or an MOI of 5 (bottom), and intracellular (left) and extracellular (right) viral titers were determined ($n = 3$, with standard errors of the means indicated by error bars).

To test whether the difference in virus release from G12 cells was due to SCG2 knockdown or premature cell death, cell viability assays were performed for T1L-infected normal, control, and G12 cells from 4 to 96 hpi (Fig. 4A). A similar trend was seen for all three cell types, indicating that virus-mediated cell death was not altered by SCG2 knockdown. Uninfected normal, control, and G12 cells were also examined by immunofluorescence microscopy (Fig. 4B). The expression of GFP in control and G12 cells confirmed successful cell transduction, and the decrease in SCG2 expression was also visible in G12 cells. G12 cells were further characterized by observation of virus protein-rich inclusions at 24 and 48 hpi (Fig. 5). Both normal and G12 cells displayed full viral infection at 24 hpi, and punctate areas of virus protein were visible at 48 hpi. A comparative complete time course at 6, 12, 18, 24, 30, and 48 hpi was performed by immunofluorescence microscopy using all three cell types, and no differences in virus protein abundance or localization were observed (data not shown).

Extracellular virus titers of both T1L and T3D are reduced in SCG2 knockdown cells. shRNA knockdown experiments were further validated by using siRNA transfection, both to validate the shRNA results and because the shRNA knockdown cells became too unstable to perform replicate experiments for statistical relevance. Optimization assays were performed with four separate and pooled siRNAs. The optimal concentration was 100 nM pooled siRNA, which provided cell viability of >90% (Fig. 6A), with a knockdown efficiency of >80% (Fig. 6B). To both validate the T1L shRNA SGC2 knockdown results and determine if the virus titer decrease in the supernatant was strain specific, we infected normal, nonsilencing control siRNA-transduced (control), or SCG2 siRNA knockdown cells with reovirus T1L, T3D Fields ($T3D^F$), or T3D Cashdollar ($T3D^C$) (Fig. 6C). Similar intracellular growth curves were seen for all three reovirus types in each cell type (Fig. 6C, left). However, all three virus types exhibited significantly lower extracellular virus titers in knockdown cells than in both normal and siRNA control cells (Fig. 6C, right).

HSV-1 extracellular virus titers are increased in SCG2 knockdown cells. To test whether SCG2 knockdown effects were virus specific, we performed similar experiments with the enveloped HSV-1. Previous studies (14–17), including our own quantitative proteomic analyses of host protein responses (18), showed that HSV-1 also grows well in HEK293 cells. Western blot analysis of HSV-1-infected HEK293 cells showed that SCG2 expression was reduced at both 6 and 24 hpi, relative to that in mock cells, and normalized to GAPDH loading control levels (Fig. 7A and B). SCG2 siRNA knockdown experiments were also performed with HSV-1. Intracellular HSV-1 titers were similar in normal, siRNA control, and SCG2 knockdown cells, but there was a significant increase in the amount of extracellular HSV-1 in SCG2 knockdown cells compared to both control cell types at 18, 24, and 48 hpi (Fig. 7C).

AP-1 activation and SCG2 expression in AP-1 knockdown, reovirus-infected cells. Different proteins in the SAPK/JNK and mitogen-activated protein kinase (MAPK) stress pathways were tested for phosphorylation-mediated activation to determine the mechanism(s) by which SCG2 was expressed and modulated by each virus (Fig. 8). HSV-1 infection induced a significant increase in SAPK/JNK and Erk phosphorylation by 24 hpi (Fig. 8A). Both reovirus strains T1L and T3D induced a slight amount of p38 phosphorylation, and HSV-1 and all reovirus strains caused SEK1/MKK4 phosphorylation at 6 hpi. To determine which monomers of the activator protein 1 (AP-1) molecule were activated, c-Fos, c-Jun, Jun-B, and Jun-D phosphorylation was examined (Fig. 8B). All reovirus strains increased c-Jun phosphorylation by 24 hpi, and $T3D^F$ and $T3D^C$ induced Jun-B phosphorylation by 24 hpi. HSV infection in-

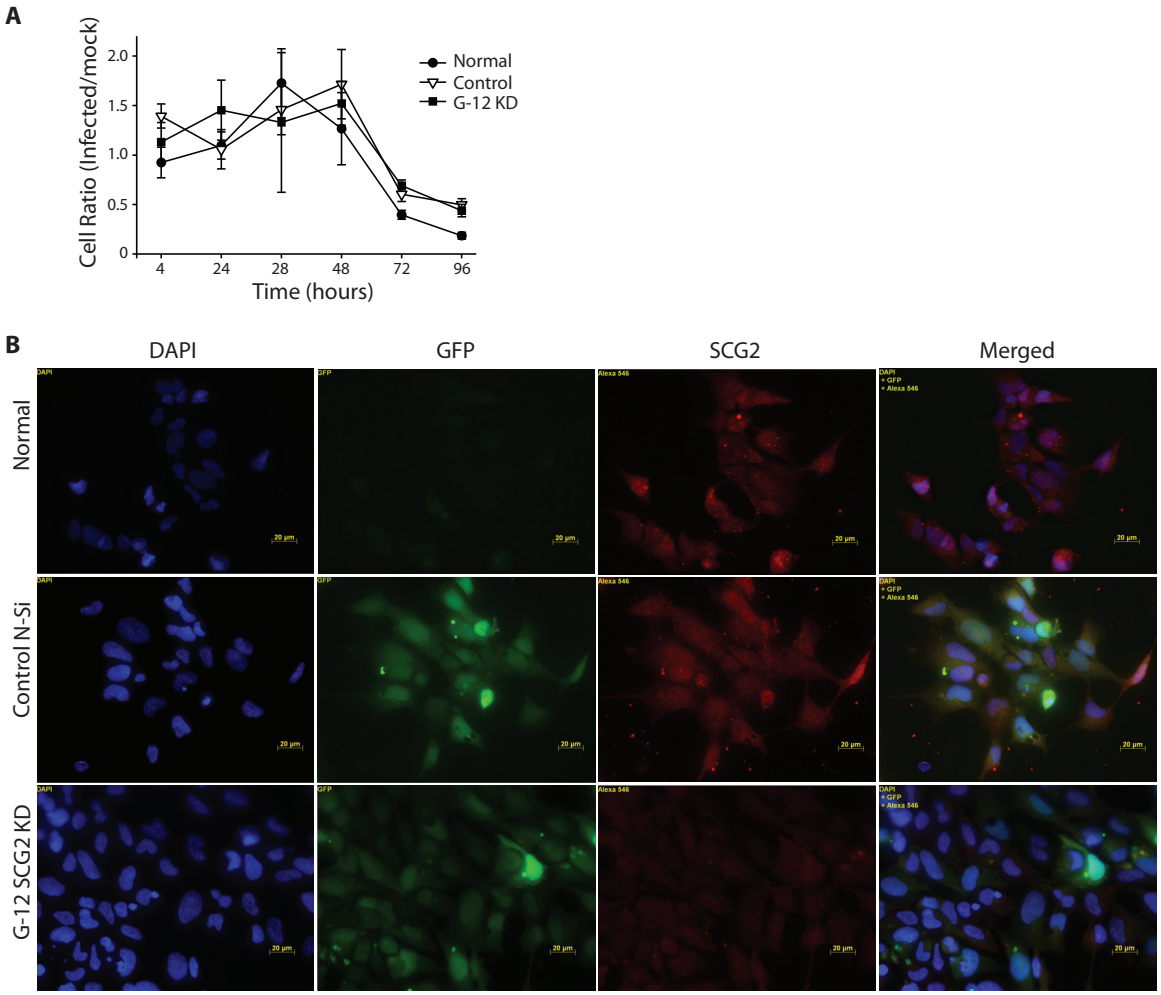

FIG 4 Characteristics of normal HEK293 cells, control nonsilencing shRNA-transduced cells, and G12-transduced SCG2 knockdown (KD) cells. (A) Cell viability of T1L-infected cells (MOI of 5) at the indicated time points postinfection, determined by a WST-1 assay. (B) Immunofluorescence microscopy analysis of staining for nuclei (DAPI), transduction (GFP), and SCG2 expression (red), with the presence of GFP in control and G12 cells providing visual confirmation of successful transduction.

duced Jun-D phosphorylation and c-Jun phosphorylation by 24 hpi. A complete list of the densitometry results, normalized to GAPDH levels in the same lanes of these Western blots, is shown in Table 2.

DISCUSSION

SCG2 is differentially regulated by reovirus and HSV infection and affects virus secretion. In the present study, we examined the possible role that SCG2 plays during virus infection. We previously showed that reovirus induces the upregulation of SCG2 late in infection (1), and another study found that the protein was downregulated ~4-fold early (0 to 3 hpi) during HSV-1 infection (19). Mechanisms underlying these dysregulations are not known. We observed both upregulation and possible phosphorylation of SCG2 beginning 18 h after reovirus T1L infection. SCG2 undergoes numerous posttranslational modifications, such as glycosylation, sulfation, and phosphorylation (20, 21). However, the function of phosphorylated SCG2 versus nonphosphorylated SCG2 is not known. The lower band might also correspond to a truncated version of the SCG2 protein after proteolysis, such as the SN peptide. Further work will need to be performed to determine if SCG2 proteolysis is also occurring postinfection. SCG2 upregulation was visible by both Western blotting and immunofluorescence analysis (Fig. 2B). Some cells did not show an increase in SCG2 staining, and the same cells also did not show evidence of infection. However, some infected cells (Fig. 2B, green arrows) also did not show an obvious increase in SCG2 expression, suggesting that SCG2 upregulation may be cell specific. Cell-specific differential responses and virus production were observed previously in populations of cultured cells (i.e., see references 22–24). Importantly, we did not observe any noninfected cells in which the SCG2 expression level was significantly higher than that in the mock-infected cultures.

SCG2 functions in the formation and packaging of cellular vesicles. Reovirus forms non-membrane-bound inclusions in the cell during viral replication and assembly. To determine if SCG2 plays a role in the formation of these viral inclusions or affects the localization of viral proteins inside the host cell, infected normal and SCG2 knockdown cells were examined by immunofluorescence microscopy (Fig. 5). Both cell types displayed a similar pres-

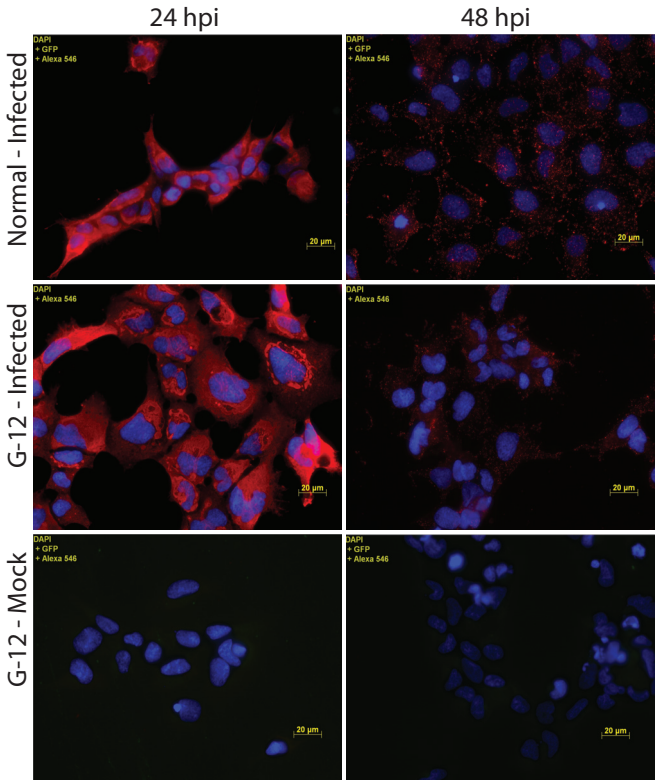

FIG 5 Characterization of T1L-infected G12 SCG2 knockdown cells. Immunofluorescence microscopic comparison of infected normal and G12 knockdown cells at 24 and 48 hpi shows virus (red) and cell nuclei (DAPI) (blue). Mock-infected (no-virus) G12 cells are shown as a control. Comparable virus protein abundances and locations are observed for both normal and infected G12 cells.

ence of the virus protein throughout the cell at 24 hpi and also showed punctate areas of virus protein at 48 hpi. The similar appearances of the virus in both cell types indicate that knocking down SCG2 does not affect the ability of the virus to form inclusion bodies and does not seem to affect viral protein localization in the cell during infection.

To further characterize the role that SCG2 plays in virus infection, we performed a series of SCG2 knockdown experiments. Both shRNA and siRNA techniques confirmed that knocking down the SCG2 protein before reovirus infection led to a decrease in the amount of virus found in the supernatant but no difference in the total amount of virus produced in the cells, indicating that SCG2 knockdown interfered with the secretion of all tested reovirus strains. To determine whether these SCG2 effects were reovirus specific or universal among different virus families, we infected the same cell type with HSV-1 and observed SCG2 expression. In contrast to our reovirus results, SCG2 was downregulated early in the HSV-1 life cycle (6 hpi). This observation agrees with previously reported findings (19). SCG2 knockdown showed an increase in the amount of secreted HSV1, the opposite effect of what was observed in reovirus infections. These results suggest that SGG2 plays different roles in the secretory pathways of nonenveloped reoviruses and the enveloped HSV (25–27).

Differential AP-1 activation by reovirus and HSV-1. Differences in the SCG2 host response to each virus type indicated that SCG2 plays a virus-specific role in virus infection; the presence of SCG2 aids in the release of reovirus but hinders HSV-1 release. The mechanism(s) by which SCG2 affects virus release is unclear, as is the mechanism of regulation of the protein in the cell during virus infection. SCG2 is targeted and regulated by AP-1 to counteract NO-mediated apoptosis as well as strongly upregulated by NO (28). SCG2 is also upregulated by extracellular signal-regulated kinase 1/2 (ERK-1/2) by a pituitary adenylate cyclase-activating polypeptide (PACAP) signaling pathway that also utilizes AP-1 for increased SCG2 gene expression (29). Activation of AP-1 by RhoA- and Rac1-dependent signaling has been observed for avian reovirus, leading to p10-mediated syncytium formation (30), but has not been identified in mammalian reovirus infections. Furthermore, HSV-1 has been shown to activate AP-1 by stimulating the p38/JNK pathway through the virion transactivator protein VP16 (31). Both viruses stimulate AP-1, and this may be due to the activation of a common pathway of host response to viral infection. It is not clear from our results why SGG2 is downregulated in HSV-1 infection, but we have shown that the opposite regulation of SCG2 by reoviruses and HSV-1 leads to an opposite effect on viral secretion, and therefore, specific mechanisms exist for each of these two viruses.

Proteins that form the AP-1 transcription factor belong to proteins of the Jun and Fos families (32). In the case of HSV-activated AP-1, the Jun-D and Jun-B proteins were mainly used in AP-1 dimerization, stimulated by p38/JNK upstream activators (31). Avian reovirus activates AP-1 and the upstream activators Rac1, RhoA, and JNK. However, the specific monomers that are activated to form AP-1 in avian reovirus infection have not been determined. p38/JNK activation is only one method of inducing transcription via AP-1, as AP-1 can be stimulated and activated by numerous cellular pathways (33, 34). We determined the activation of some of these proteins, specifically in the p38/JNK pathway, by observing phosphorylation of these proteins in both HSV and mammalian reovirus infections (Fig. 8). The proteins JNK, Erk, and p38 are the main signaling proteins that mediate the MAPK pathway, and SEK/MKK4 is an upstream signaling protein of this pathway (35, 36). At the early 6-h time point, HSV caused phosphorylation of SEK1/MKK4 (Fig. 8A). Expectedly, by 24 hpi, JNK was highly phosphorylated by HSV infection, correlating with previously reported results (31). For mammalian reovirus, there was phosphorylation of SEK/MKK4 at the 6-h time point for T1L and $T3D^F$; however, there was no phosphorylation of JNK or Erk. There was slight phosphorylation of p38 (1.6- to 1.8-fold increase compared to mock infection) for T1L and $T3D^F$ reoviruses, which may lead to downstream AP-1 activation. This indicates that mammalian reovirus activates AP-1 by a different mechanism than that of avian reoviruses. Avian reoviruses activate RhoA and Rac1 by the viral p10 protein, a protein that is not encoded by mammalian reoviruses (37). To determine which of the monomer proteins comprise the active AP-1 protein for each infection, we tested for the phosphorylation of the c-Fos, c-Jun, Jun-B, and Jun-D proteins (Fig. 8B). The c-Fos protein was not phosphorylated for any of our virus infections; however, the c-Jun protein was phosphorylated by all three reovirus types. Jun-B was also phosphorylated heavily by the $T3D^F$ and $T3D^C$ subtypes, but not by T1L, indicating differences in the mechanism of AP-1 activation among virus subtypes. Finally, Jun-D was phosphorylated by HSV infection, which correlates with findings reported previously (31).

A proposed mechanism for SCG2 expression is shown in Fig. 9.

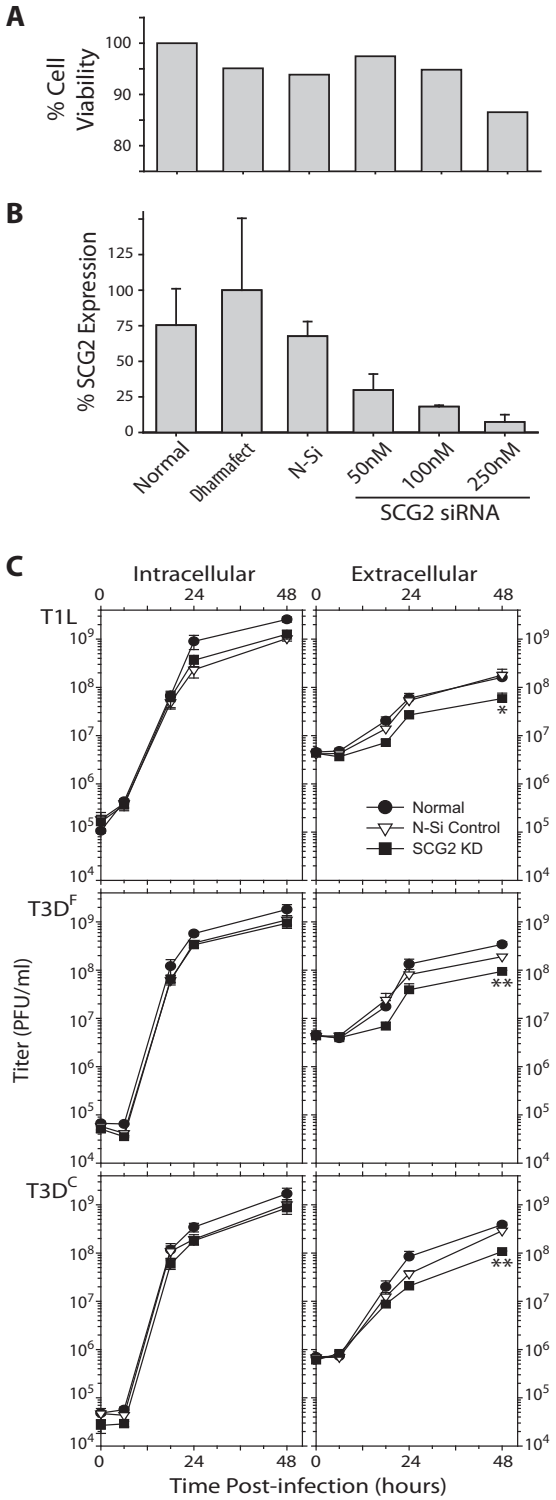

FIG 6 Normal, nonsilencing control siRNA-treated, and pooled-siRNA-treated SCG2 knockdown cells were optimized and infected with reovirus T1L, $T3D^F$, or $T3D^C$. (A) Cell viability of normal cells, Dharmafect-1-treated cells, nonsilencing control (N-Si) siRNA-treated cells, and HEK293 cells treated with pooled SCG2 siRNA at the indicated concentrations, determined by a WST-1 assay. (B) SCG2 protein expression in each type of cell, normalized to the GAPDH levels in the same lanes and to levels in Dharmafect-1-treated cells. (C) Growth assays with reovirus T1L (top), T3D-Fields (middle), and T3D-Cashdollar (bottom) in SCG2 knockdown cells, with intracellular (left) and extracellular (right) viral titers being determined by a plaque assay at the indicated times postinfection ($n = 3$, with standard errors of the means indicated by error bars). Significantly smaller amounts of extracellular virus were seen for knockdown cells than for normal and nonsilencing control cells (*, $P < 0.005$; **, $P < 0.0005$ [determined by analysis of variance]).

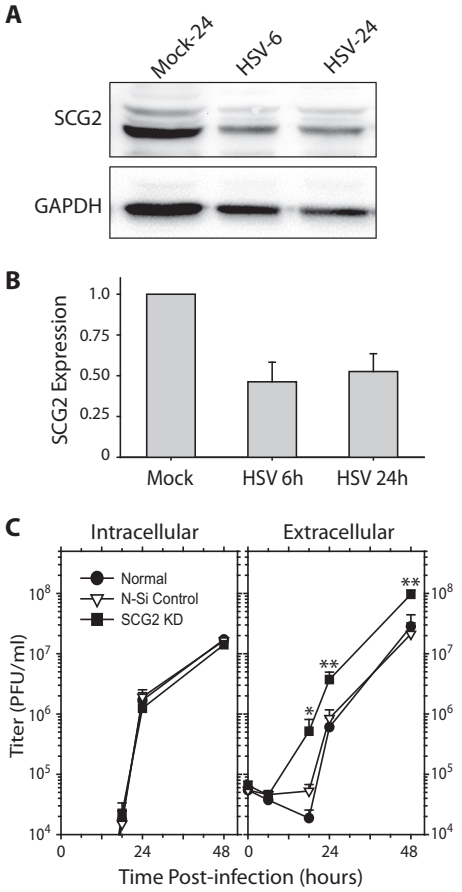

FIG 7 Characterization of SCG2 in HSV-1-infected HEK293 cells. (A) Representative immunoblot of SCG2 and GAPDH in HEK293 cells either mock infected or infected with HSV-1 at an MOI of 5 at 6 and 24 hpi. (B) Densitometric determination of SCG2 expression levels, normalized to the GAPDH levels in the same lanes and to levels with mock treatment ($n = 3$, with standard errors of the means indicated by error bars). (C) Growth assays of HSV-1 in normal, nonsilencing (N-Si) control, and SCG2 knockdown cells. Intracellular (left) and extracellular (right) HSV-1 titers were determined at the indicated time points ($n = 3$, with standard errors of the means indicated by error bars). Titers were below the limit of detection (100 PFU) for intracellular 0- and 6-h time points. Significantly higher extracellular HSV-1 titers were observed for knockdown cells than for normal and nonsilencing control cells at multiple time points (*, $P < 0.05$; **, $P < 0.005$).

Previous studies showed that avian reoviruses phosphorylate JNK with different upstream activators, and the dimers used for AP-1 in this instance are unknown (30). Mammalian reoviruses activate MKK4 but not JNK. Therefore, MKK4 may activate AP-1 by alternate proteins, such as p38, and utilize the c-Jun and Jun-B monomers to form heterodimers as active AP-1 molecules. SCG2 upregulation occurred much later in infection (18 hpi) than did SCG2 downregulation in HSV infection. This is due to the time that it takes for the virus to replicate and produce virus proteins in the host cell that will lead to the activation of AP-1. For HSV-1, it

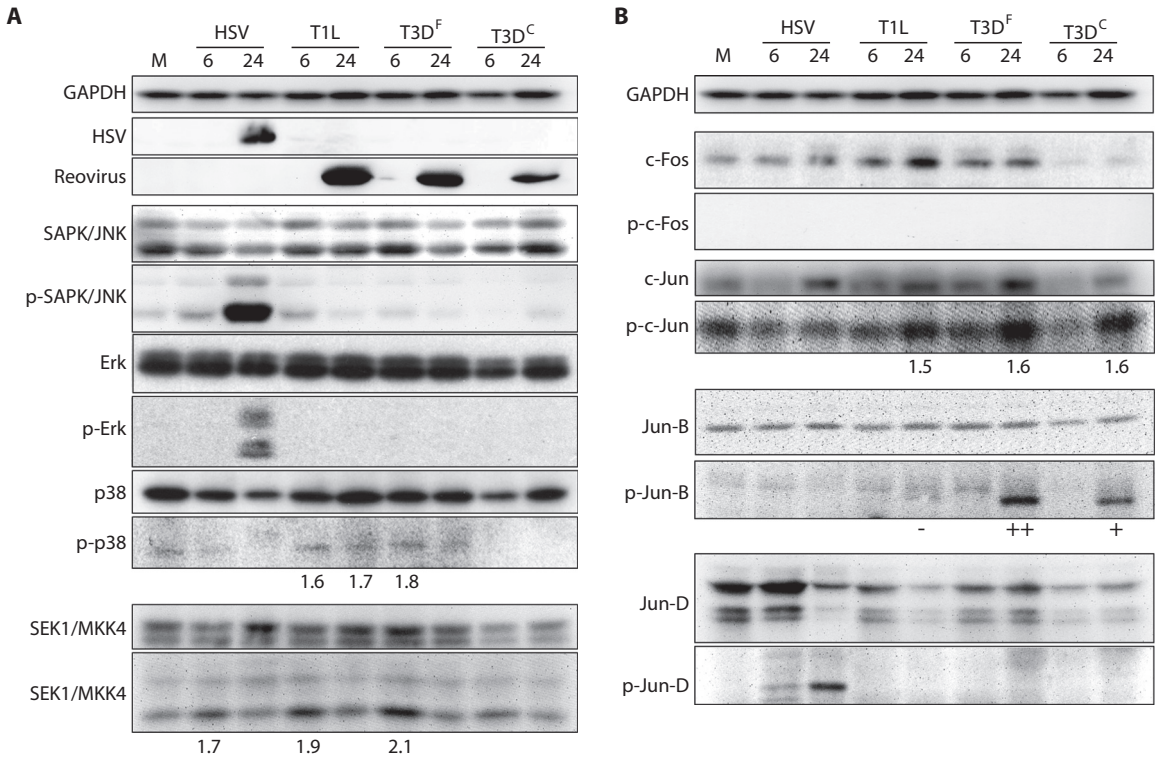

FIG 8 Activation of SAPK/JNK and MAPK proteins in mock-infected (M), HSV-1-infected, reovirus T1L-infected, reovirus $T3D^F$-infected, and reovirus $T3D^C$-infected cells at 6 hpi and 24 hpi. Densitometry analysis was performed on bands, results were compared to those for mock treatment, and values are shown below the corresponding blots. −, +, and ++ represent no, low, and high phospho-Jun-B signals, respectively. All such comparative values are shown in Table 2. (A) Upstream protein activation of SAPK/JNK and MAPK proteins was tested for phosphorylation of JNK, Erk, p38, and MKK4 proteins. (B) AP-1 monomer proteins were tested for activation by phosphorylation of c-Fos, c-Jun, Jun-B, and Jun-D proteins.

was previously shown that HSV-1 activates AP-1 early during virus infection (31), which is known to regulate SCG2 expression (28, 29, 38). The tegument protein VP16 causes this activation (31). Our experiments confirmed the activation of both the JNK and Jun-D proteins during HSV1 infection, which is known to lead to AP-1 activation. Additional data are needed to elucidate the pathway of SCG2 downregulation, and therefore, in the model, we can incorporate only the observation that HSV-1 infec-

TABLE 2 Densitometry results for AP-1 signaling pathway proteins during virus infection[a]

Protein	Protein level								
	Mock treatment	HSV		T1L		$T3D^F$		$T3D^C$	
		6 hpi	24 hpi	6 hpi	24 hpi	6 hpi	24 hpi	6 hpi	24 hpi
SAPK/JNK	1.00	0.60	0.54	0.60	0.50	0.58	0.41	0.57	0.64
p-SAPK/JNK	1.00	1.82	11.51	2.48	0.57	0.61	0.27	0.29	0.53
Erk	1.00	0.94	0.66	0.90	1.04	0.90	0.77	0.76	0.90
p-Erk	−	−	++	−	−	−	−	−	−
p38	1.00	0.84	0.49	0.70	0.94	0.77	0.70	0.60	0.68
p-p38	1.00	0.47	0.49	1.60	1.72	1.83	0.73	0.07	0.06
SEK1/MKK4	1.00	0.87	0.82	0.98	1.20	1.08	0.77	0.61	0.68
p-SEK1/MKK4	1.00	1.66	0.86	1.85	1.47	2.12	1.01	1.58	0.84
c-Fos	1.00	1.08	1.40	1.63	3.01	1.74	1.76	0.35	0.31
p-c-Fos	−	−	−	−	−	−	−	−	−
c-Jun	1.00	0.88	1.66	1.07	1.61	1.47	1.68	1.33	1.10
p-c-Jun	1.00	0.84	1.18	0.73	1.52	1.11	1.62	0.94	1.56
Jun-B	1.00	0.91	0.97	0.96	1.13	1.15	1.00	0.59	0.87
p-Jun-B	−	−	−	−	−	−	++	−	+
Jun-D	1.00	1.33	0.54	0.62	0.36	0.66	0.72	0.40	0.40
p-Jun-D	−	+	++	−	−	−	−	−	−

[a] Values in the table represent the fold change of respective proteins in the various virus-infected samples compared to mock levels and were normalized to the GAPDH levels within the same lanes and to mock levels. Note that protein abundances that cannot be calculated because there was no signal for the mock treatment for comparison are designated by either a "−" for no signal, a "+" for a low signal, or a "++" for a high signal.

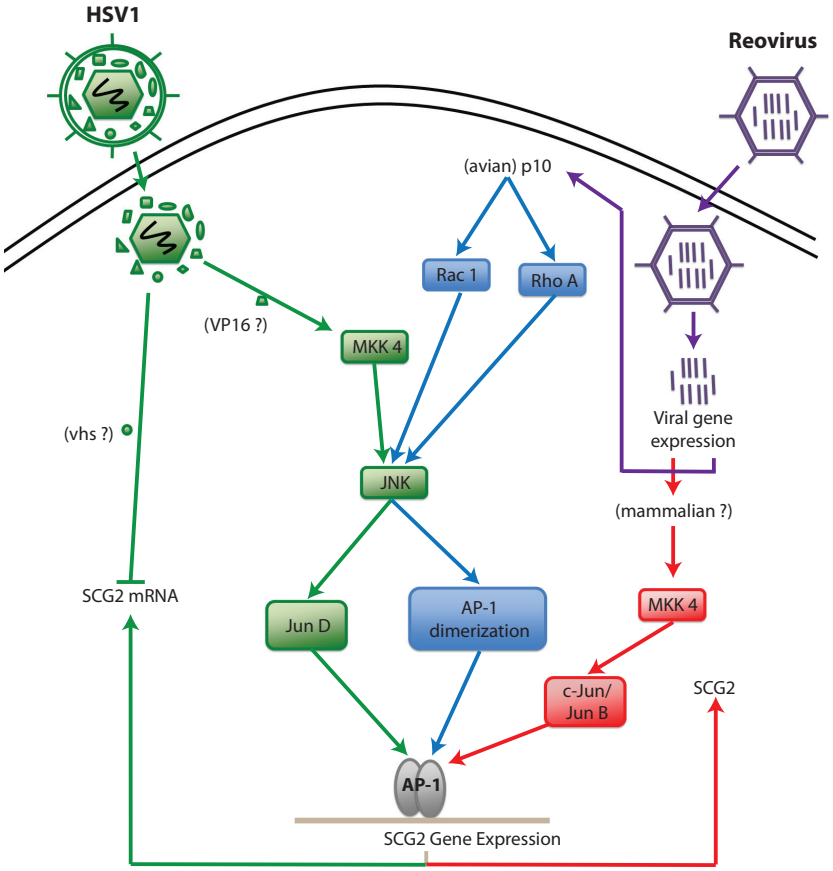

FIG 9 Proposed mechanism for SCG2 expression in HSV- and reovirus-infected cells. Known avian reovirus AP-1 activation pathway molecules are shown in purple and blue. The proposed mammalian reovirus pathway is shown in red. The HSV signaling pathway is shown in green (based upon data reported in the literature and in this study).

tion enhances MKK4 phosphorylation and reduces the level of SGG2. However, since both AP-1 activation (31) and SCG2 down-regulation occur at early times in HSV-1 infection, we hypothesize that the tegument activator protein VP16 may be responsible for activating JNK and the AP-1 pathway through MKK4, while the virus host shutoff protein, which is known to degrade host mRNA (38–40) and is also carried into the cell within the HSV-1 tegument, may cause the early degradation of SGG2 mRNA.

Conclusions. Secretogranin II regulation during virus infection affects the amount of virus that is released from the cell. SCG2 expression during infection is regulated through the activation of the AP-1 transcription pathway. However, the precise mechanism by which SCG2 affects virus secretion remains unknown. SCG2 is affected in a virus-specific manner: the direction in which it is regulated, whether up or down, depends on the virus type, and the specific AP-1 activation pathway is also virus dependent. Further delineation of the role that SCG2 plays during virus infection will lead to a greater understanding of virus-host interactions and the mechanisms that contribute to virus release.

ACKNOWLEDGMENT

This work was supported by Canadian Institutes of Health Research (CIHR) grant MOP-11630.

REFERENCES

1. **Berard AR, Cortens JP, Krokhin O, Wilkins JA, Severini A, Coombs KM.** 2012. Quantification of the host response proteome after mammalian reovirus T1L infection. PLoS One **7:**e51939. http://dx.doi.org/10.1371/journal.pone.0051939.
2. **Bartolomucci A, Possenti R, Mahata SK, Fischer-Colbrie R, Loh YP, Salton SRJ.** 2011. The extended granin family: structure, function, and biomedical implications. Endocr Rev **32:**755–797. http://dx.doi.org/10.1210/er.2010-0027.
3. **Montero-Hadjadje M, Vaingankar S, Elias S, Tostivint H, Mahata SK, Anouar Y.** 2008. Chromogranins A and B and secretogranin II: evolutionary and functional aspects. Acta Physiol **192:**309–324.
4. **Helle KB.** 2010. Chromogranins A and B and secretogranin II as prohormones for regulatory peptides from the diffuse neuroendocrine system. Results Probl Cell Differ **50:**21–44. http://dx.doi.org/10.1007/400_2009_26.
5. **Beuret N, Stettler H, Renold A, Rutishauser J, Spiess M.** 2004. Expression of regulated secretory proteins is sufficient to generate granule-like structures in constitutively secreting cells. J Biol Chem **279:**20242–20249. http://dx.doi.org/10.1074/jbc.M310613200.
6. **Courel M, Vasquez MS, Hook VY, Mahata SK, Taupenot L.** 2008. Sorting of the neuroendocrine secretory protein secretogranin II into the regulated secretory pathway—role of N- and C-terminal alpha-helical domains. J Biol Chem **283:**11807–11822. http://dx.doi.org/10.1074/jbc.M709832200.
7. **Desmoucelles C, Vaudry H, Eiden LE, Anouar Y.** 1999. Synergistic action of upstream elements and a promoter-proximal CRE is required for neuroendocrine cell-specific expression and second-messenger regulation of the gene encoding the human secretory protein secretogranin II. Mol Cell Endocrinol **157:**55–66. http://dx.doi.org/10.1016/S0303-7207(99)00158-6.
8. **Boutahricht M, Guillemot J, Montero-Hadjadje M, Barakat Y, El Ouezzani S, Alaoui A, Yon L, Vaudry H, Anouar Y, Magoul R.** 2007. Immunohistochemical distribution of the secretogranin II-derived peptide EM66 in the rat hypothalamus: a comparative study with jerboa. Neurosci Lett **414:**268–272. http://dx.doi.org/10.1016/j.neulet.2006.12.033.

9. **Ida-Eto M, Nomura M, Ohkawara T, Narita N, Narita M.** 2014. Localization of manserin, a secretogranin II-derived neuropeptide, in the oviduct of female rats. Acta Histochem **116:**522–526. http://dx.doi.org/10.1016/j.acthis.2013.11.009.
10. **Shooshtarizadeh P, Zhang D, Chich JF, Gasnier C, Schneider F, Haikel Y, Aunis D, Metz-Boutigue MH.** 2010. The antimicrobial peptides derived from chromogranin/secretogranin family, new actors of innate immunity. Regul Pept **165:**102–110. http://dx.doi.org/10.1016/j.regpep.2009.11.014.
11. **Berard A, Coombs KM.** 2009. Mammalian reoviruses: propagation, quantification, and storage. Curr Protoc Microbiol Chapter 15: Unit15C.1. http://dx.doi.org/10.1002/9780471729259.mc15c01s14.
12. **Coombs KM, Berard A, Xu W, Krokhin O, Meng X, Cortens JP, Kobasa D, Wilkins J, Brown EG.** 2010. Quantitative proteomic analyses of influenza virus-infected cultured human lung cells. J Virol **84:**10888–10906. http://dx.doi.org/10.1128/JVI.00431-10.
13. **Tran AT, Cortens JP, Du Q, Wilkins JA, Coombs KM.** 2013. Influenza virus induces apoptosis via BAD-mediated mitochondrial dysregulation. J Virol **87:**1049–1060. http://dx.doi.org/10.1128/JVI.02017-12.
14. **Erlandsson AC, Bladh LG, Stierna P, Yucel-Lindberg T, Hammarsten O, Modeer T, Harmenberg J, Wikstrom AC.** 2002. Herpes simplex virus type 1 infection and glucocorticoid treatment regulate viral yield, glucocorticoid receptor and NF-kappa B levels. J Endocrinol **175:**165–176. http://dx.doi.org/10.1677/joe.0.1750165.
15. **Jurak I, Kramer MF, Mellor JC, van Lint AL, Roth FP, Knipe DM, Coen DM.** 2010. Numerous conserved and divergent microRNAs expressed by herpes simplex viruses 1 and 2. J Virol **84:**4659–4672. http://dx.doi.org/10.1128/JVI.02725-09.
16. **Bedadala GR, Palem JR, Graham L, Hill JM, McFerrin HE, Hsia SC.** 2011. Lytic HSV-1 infection induces the multifunctional transcription factor early growth response-1 (EGR-1) in rabbit corneal cells. Virol J **8:**262. http://dx.doi.org/10.1186/1743-422X-8-262.
17. **Schumacher AJ, Mohni KN, Kan YN, Hendrickson EA, Stark JM, Weller SK.** 2012. The HSV-1 exonuclease, UL12, stimulates recombination by a single strand annealing mechanism. PLoS Pathog **8:**e1002862. http://dx.doi.org/10.1371/journal.ppat.1002862.
18. **Berard AR, Coombs KM, Severini A.** 2015. Quantification of the host response proteome after herpes simplex 1 virus infection. J Proteome Res **14:**2121–2142. http://dx.doi.org/10.1021/pr5012284.
19. **Ray N, Enquist LW.** 2004. Transcriptional response of a common permissive cell type to infection by two diverse alphaherpesviruses. J Virol **78:**3489–3501. http://dx.doi.org/10.1128/JVI.78.7.3489-3501.2004.
20. **Dillen L, Miserez B, Claeys M, Aunis D, Depotter W.** 1993. Posttranslational processing of proenkephalins and chromogranins secretogranins. Neurochem Int **22:**315–352. http://dx.doi.org/10.1016/0197-0186(93)90016-X.
21. **Rosa P, Mantovani S, Rosboch R, Huttner WB.** 1992. Monensin and brefeldin-A differentially affect the phosphorylation and sulfation of secretory proteins. J Biol Chem **267:**12227–12232.
22. **Zhu Y, Yongky A, Yin J.** 2009. Growth of an RNA virus in single cells reveals a broad fitness distribution. Virology **385:**39–46. http://dx.doi.org/10.1016/j.virol.2008.10.031.
23. **Timm A, Yin J.** 2012. Kinetics of virus production from single cells. Virology **424:**11–17. http://dx.doi.org/10.1016/j.virol.2011.12.005.
24. **Schulte MB, Andino R.** 2014. Single-cell analysis uncovers extensive biological noise in poliovirus replication. J Virol **88:**6205–6212. http://dx.doi.org/10.1128/JVI.03539-13.
25. **Matis J, Kudelova M.** 2001. Early shutoff of host protein synthesis in cells infected with herpes simplex viruses. Acta Virol **45:**269–277.
26. **Shiflett LA, Read GS.** 2013. mRNA decay during herpes simplex virus (HSV) infections: mutations that affect translation of an mRNA influence the sites at which it is cleaved by the HSV virion host shutoff (Vhs) protein. J Virol **87:**94–109. http://dx.doi.org/10.1128/JVI.01557-12.
27. **Dauber B, Saffran HA, Smiley JR.** 2014. The herpes simplex virus 1 virion host shutoff protein enhances translation of viral late mRNAs by preventing mRNA overload. J Virol **88:**9624–9632. http://dx.doi.org/10.1128/JVI.01350-14.
28. **Li L, Hung AC, Porter AG.** 2008. Secretogranin II: a key AP-1-regulated protein that mediates neuronal differentiation and protection from nitric oxide-induced apoptosis of neuroblastoma cells. Cell Death Differ **15:**879–888. http://dx.doi.org/10.1038/cdd.2008.8.
29. **Turquier V, Yon L, Grumolato L, Alexandre D, Fournier A, Vaudry H, Anouar Y.** 2001. Pituitary adenylate cyclase-activating polypeptide stimulates secretoneurin release and secretogranin II gene transcription in bovine adrenochromaffin cells through multiple signaling pathways and increased binding of pre-existing activator protein-1-like-transcription factors. Mol Pharmacol **60:**42–52.
30. **Liu HJ, Lin PY, Wang LR, Hsu HY, Liao MH, Shih WL.** 2008. Activation of small GTPases RhoA and Rac1 is required for avian reovirus p10-induced syncytium formation. Mol Cells **26:**396–403.
31. **Zachos G, Clements B, Conner J.** 1999. Herpes simplex virus type 1 infection stimulates p38/c-Jun N-terminal mitogen-activated protein kinase pathways and activates transcription factor AP-1. J Biol Chem **274:**5097–5103. http://dx.doi.org/10.1074/jbc.274.8.5097.
32. **Bakiri L, Matsuo K, Wisniewska M, Wagner EF, Yaniv M.** 2002. Promoter specificity and biological activity of tethered AP-1 dimers. Mol Cell Biol **22:**4952–4964. http://dx.doi.org/10.1128/MCB.22.13.4952-4964.2002.
33. **Angel P, Karin M.** 1991. The role of Jun, Fos and the Ap-1 complex in cell-proliferation and transformation. Biochim Biophys Acta **1072:**129–157.
34. **Karin M.** 1995. The regulation of Ap-1 activity by mitogen-activated protein kinases. J Biol Chem **270:**16483–16486. http://dx.doi.org/10.1074/jbc.270.28.16483.
35. **Johnson GL, Lapadat R.** 2002. Mitogen-activated protein kinase pathways mediated by ERK, JNK, and p38 protein kinases. Science **298:**1911–1912. http://dx.doi.org/10.1126/science.1072682.
36. **Haeusgen W, Herdegen T, Waetzig V.** 2011. The bottleneck of JNK signaling: molecular and functional characteristics of MKK4 and MKK7. Eur J Cell Biol **90:**536–544. http://dx.doi.org/10.1016/j.ejcb.2010.11.008.
37. **Attoui H, Mertens PPC, Becnel J, Belaganahalli S, Bergoin M, Brussaard CP, Chappell JD, Ciarlet M, Del Vas M, Dermody TS, Dormitzer PR, Duncan R, Fang Q, Graham R, Guglielmi KM, Harding RM, Hillman B, Makkay A, Marzachi C, Matthijnssens J, Milne RG, Mohd Jaafar F, Mori H, Noordeloos AA, Omura T, Patton JT, Rao S, Maan M, Stoltz D, Suzuki N, Upadhyaya NM, Wei C, Zhou H.** 2011. Reoviridae, p 541–637. *In* King AMQ, Adams MJ, Carstens EB, Lefkowitz EJ (ed), Virus taxonomy: classification and nomenclature of viruses. Ninth report of the International Committee on Taxonomy of Viruses. Academic Press, London, United Kingdom.
38. **Esclatine A, Taddeo B, Evans L, Roizman B.** 2004. The herpes simplex virus 1 U(L)41 gene-dependent destabilization of cellular RNAs is selective and may be sequence-specific. Proc Natl Acad Sci U S A **101:**3603–3608. http://dx.doi.org/10.1073/pnas.0400354101.
39. **Kwong AD, Frenkel N.** 1987. Herpes simplex virus-infected cells contain a function(s) that destabilizes both host and viral mRNAs. Proc Natl Acad Sci U S A **84:**1926–1930. http://dx.doi.org/10.1073/pnas.84.7.1926.
40. **Shu MF, Taddeo B, Roizman B.** 2015. Tristetraprolin recruits the herpes simplex virion host shutoff RNase to AU-rich elements in stress response mRNAs to enable their cleavage. J Virol **89:**5643–5650. http://dx.doi.org/10.1128/JVI.00091-15.